A nonstationary ENSO-NAO relationship due to AMO modulation

Article

Accepted Version

A Nonstationary ENSO-NAO relationship due to AMO modulation

Wenjun Zhang[1], Xuebin Mei[1], Xin Geng[1], Andrew G. Turner[2,3], Fei-Fei Jin[4]

[1]CIC-FEMD/ILCEC, Key Laboratory of Meteorological Disaster of Ministry of Education, Nanjing University of Information Science and Technology, Nanjing 210044, China

[2]National Center for Atmospheric Science, University of Reading, Reading RG6 6BB, UK

[3]Department of Meteorology, University of Reading, Reading RG6 6BB, UK

[4]Department of Atmospheric Sciences, SOEST, University of Hawai'i at Manoa, Honolulu, HI 96822, USA

Jun 2, 2018

(*Submitting to Journal of Climate*)

Corresponding author address:
Dr. Wenjun Zhang
College of Atmospheric Sciences, Nanjing University of Information Science and Technology, Nanjing 210044, China.
E-mail: zhangwj@nuist.edu.cn

Abstract

Many previous studies have demonstrated a high uncertainty in the relationship between the El Niño-Southern Oscillation (ENSO) and North Atlantic Oscillation (NAO). In the present work, decadal modulation by the Atlantic Multidecadal Oscillation (AMO) is investigated as a possible cause of the nonstationary ENSO-NAO relationship based on observed and reanalysis data. It is found that the negative ENSO-NAO correlation in late winter is significant only when ENSO and the AMO are in-phase (AMO+/El Niño and AMO-/La Niña). However, no significant ENSO-driven atmospheric anomalies can be observed over the North Atlantic when ENSO and the AMO are out-of-phase (AMO-/El Niño and AMO+/La Niña). Further analysis indicates that the sea surface temperature anomaly (SSTA) in the tropical North Atlantic (TNA) plays an essential role in this modulating effect. Due to broadly analogous TNA SSTA responses to both ENSO and the AMO during late winter, a warm SSTA in the TNA is evident when El Niño occurs during a positive AMO phase, resulting in a significantly weakened NAO, and vice versa when La Niña occurs during a negative AMO phase. In contrast, neither the TNA SSTA nor the NAO show a prominent change under out-of-phase combinations of ENSO and AMO. The AMO modulation and associated effect of the TNA SSTA are shown to be well reproduced by historical simulations of the HadCM3 coupled model and further verified by forced experiments using an atmospheric circulation model. These offer hope that similar models will be able to make predictions for the NAO when appropriately initialized.

1. Introduction

As the dominant low-frequency atmospheric circulation variability in the extratropical Northern Hemisphere, the North Atlantic Oscillation (NAO) has extensive and pronounced climate impacts around the globe (e.g., Hurrell 1995, 2003; Cattiaux et al. 2010; Cohen et al. 2012; Li et al. 2013, 2018). The NAO explains much of the observed temperature variability over Eurasia and North America (e.g., Hurrell 1996; Wang et al. 2010), and its decadal variation also plays a role in the recent decline of Arctic sea ice concentration (Deser and Teng 2008). To date, more and more attention has been paid to understanding NAO variability and its drivers in order to improve seasonal-to-interannual prediction of the NAO itself and associated impacts (e.g., Johansson 2007; Dunstone et al. 2016; Smith et al. 2016). On interannual timescales, possible influences of the El Niño-Southern Oscillation (ENSO) on the NAO have been extensively studied, since ENSO is one of the largest modes of interannual variability in the coupled Earth system.

ENSO exerts its influence on the global climate mostly through so-called atmospheric bridge mechanisms (e.g., Klein et al. 1999; Alexander et al. 2002; Lau and Nath 2003; Graf and Zanchettin 2012; Zhang et al. 2015). While the climate responses to ENSO in the North Pacific and North America regions are well understood (e.g., Hoskins and Karoly 1981; Wallace and Gutzler 1981; Infanti and Kirtman 2016), the physical linkages between ENSO and climate variability over the North Atlantic-European sector are still unclear. Early studies argued that signals of ENSO are almost absent in North Atlantic/European climate variability (e.g.,

62 Ropelewski and Halpert 1987; Halpert and Ropelewski 1992). This viewpoint is
63 challenged by subsequent studies, which demonstrated an ENSO signal in Europe
64 albeit with large inter-event diversity (e.g., Fraedrich 1994; Gouirand and Moron
65 2003; Brönnimann et al. 2007a,b), possibly due to the existence of two types of
66 ENSO (Graf and Zanchettin 2012; Zhang et al. 2015, 2018) and prominent
67 sub-seasonal variations (e.g., Fraedrich and Muller 1992; Moron and Gouirand 2003;
68 Geng et al. 2017). Various observational and modeling studies have demonstrated that
69 El Niño events usually coincide with a negative NAO-like atmospheric anomaly
70 pattern during the late winter season, with a colder and drier than normal climate over
71 Northern Europe (e.g., Mathieu et al. 2004; Brönnimann et al. 2007a,b). The
72 responses to La Niña events are approximately opposite in sign to those of El Niño.
73 Nevertheless, the dynamical mechanisms addressing how ENSO-related tropical sea
74 surface temperature (SST) anomalies (SSTA) influence the NAO variability are still
75 under debate. It has been proposed that the atmosphere over the North Pacific may
76 serve as a bridge linking ENSO-associated diabatic heating in the tropical Pacific with
77 atmospheric circulation anomalies over the North Atlantic (e.g., Wu and Hsieh 2004;
78 Graf and Zanchettin 2012; Zhang et al. 2015, 2018). ENSO-forced synoptic eddies
79 over the eastern Pacific and North America could modulate the meridional
80 propagation of synoptic wave packets over the North Atlantic, and then favor the
81 occurrence of different NAO phases (e.g., Li and Lau 2012a, b; Drouard et al. 2015).
82 The stratosphere might also act as a mediator to connect the signal between the
83 Pacific and Atlantic basins (e.g., Castanheira and Graf 2003; Ineson and Scaife 2009;

84 Bell et al. 2009). As an additional pathway, some previous studies reported that the
85 delayed tropical Atlantic SSTA following the ENSO peak could also affect the North
86 Atlantic atmospheric circulation (e.g., Watanabe and Kimoto 1999; Robertson et al.
87 2000; Peng et al. 2005; Li et al. 2007; Davini et al. 2015).

88 Many studies show that the NAO also displays prominent decadal variability,
89 which may be associated with the underlying low-frequency SST forcing. In particular,
90 the linkage between the NAO and the Atlantic multidecadal oscillation (AMO; Peings
91 and Magnusdottir 2014; Omrani et al. 2014) has been widely explored, since the
92 AMO has been recognized as an important driver of Northern Hemisphere climate
93 variability (e.g., Kerr 2000; Enfield et al. 2001; Zhang et al. 2007; Sun et al. 2011;
94 Sun et al. 2015). A warm AMO phase usually accompanies occurrence of more
95 frequent negative NAO and thus more cold days over Europe and North America (e.g.,
96 Ting et al. 2011, 2014; Kavvada et al. 2013; Peings and Magnusdottir 2014).
97 Therefore, it is compelling to hypothesize that the AMO may in some way act to
98 modulate the ENSO-NAO relationship.

99 Since any modulation of the ENSO-NAO relationship by the AMO has not been
100 sufficiently elucidated in the aforementioned studies, in this study we investigate the
101 influence of phase combinations of the ENSO and AMO on the NAO based on
102 long-term observational datasets and model simulations. Our results will show that the
103 AMO causes significant modulation of the ENSO-NAO relationship. Furthermore, the
104 physical mechanisms behind this AMO modulation effect are also proposed. In the
105 remainder of the paper, Section 2 introduces the observational datasets, model

106 simulations and methodologies. The modulation effect of the ENSO-NAO
107 relationship by the AMO is illustrated in Section 3. In Section 4, we propose the
108 possible mechanisms for modulation, and further use historical HadCM3 model
109 simulations as well as atmospheric general circulation model (AGCM) experiments
110 based on Geophysical Fluid Dynamics Laboratory (GFDL) global Atmospheric
111 Model version 2.1 (AM2.1) to validate our hypotheses. Finally, a summary and
112 discussion of the results are presented in Section 5.
113

114 ## 2. Datasets and Methods and experimental design

115 ### 2.1 Datasets and Methods

116 The monthly datasets used in this study include global SST derived from the
117 National Oceanic and Atmospheric Administration (NOAA) Extended Reconstructed
118 SST analysis, version 3 (ERSST v3b) from 1950 to 2016 (Smith et al. 2008).
119 Atmospheric circulations are examined based on the National Environmental
120 Prediction Center/National Center for the Atmospheric Research (NCEP/NCAR)
121 monthly reanalysis data from 1950 to 2016 (Kalnay et al. 1996) and Twentieth
122 Century Reanalysis (20CR) monthly data from 1900 to 2012 (Compo et al. 2010). To
123 describe the NAO-associated atmospheric activity, the NAO index is defined as the
124 difference in normalized zonal-averaged sea-level pressure (SLP) over the North
125 Atlantic region (80°W-30°E) between 35°N and 65°N (Li et al. 2003). The AMO
126 index is calculated as the area-averaged SSTA over the North Atlantic region
127 (0°-60°N, 0°-80°W) (Trenberth and Shea 2006).

ENSO events usually reach their peak during boreal winter (December-January-February, DJF), and the relatively stable NAO response to ENSO is found mainly during the late winter (January-February-March, JFM) (e.g., Zhang et al. 2015, 2018). Thus, we use the DJF Niño3.4 index (SSTA averaged over 5°S-5°N and 120°-170°W) as a measure of ENSO events and the JFM NAO index to characterize NAO variability. The DJF AMO is also employed (other seasonal means computed for the AMO index such as JFM or DJFM do not change the conclusion). To better isolate the inherent decadal signal of the AMO, we extract its low-frequency variability by using a 10-year low-pass fast Fourier transform (FFT) filter (other filters for the AMO index such as 9-year and 11-year low-pass filter do not change the conclusion). The linear trends of all data were removed to avoid possible influences associated with global warming. A threshold of ±0.5 standard deviations of the Niño3.4 index is used to define ENSO events. With this method we identify 20 El Niño and 24 La Niña winters (Table 1). The year in Table 1 corresponds to year(0)/year(1), which denotes the ENSO developing and decaying years, respectively. All statistical significance tests were performed based on the two-tailed Student's *t*-test.

We also analyze the Hadley Centre coupled model version 3 (HadCM3) output (1860-2005) to further verify the AMO modulation on the ENSO-NAO relationship. The model simulation, known as a "historical experiment", was driven by prescribed historical climate forcing, which includes changing atmospheric composition, solar forcing, and land use (Taylor et al. 2012). We chose the HadCM3 simulation in this

study since the model has the capability to simulate both the AMO and ENSO (e.g., Lu et al. 2006; Dong et al. 2006). Since HadCM3 is a coupled model, we do not expect the phases of AMO and ENSO within it to coincide with those in observations over the 20th century; any memory of the initial state will be lost within a few years of the start of the integration.

2.2 Experimental design

In order to examine the AMO-modulation effect on the ENSO-NAO relationship, we conducted several modeling experiments based on the GFDL AM2.1 (The GFDL Global Atmospheric Model Development Team 2004) with a horizontal resolution of 2.5° longitude × 2° latitude. As a reference state, global climatological (monthly varying) SST was used to force the atmospheric model (CTRL). In addition, a group of sensitivity experiments (PAEL, NAEL, PALA and NALA) was designed (Table 2). To inspect the combined influence of the ENSO and AMO, in the PAEL experiment we added the composite SSTA for the AMO+/El Niño case on the monthly climatological SST from December to March in the tropical Pacific (30°S-30°N, 120°E-90°W) and TNA (0-30°N, 80°W-0) region (Table 2). The other three experiments (PALA, NAEL, NALA) are the same as the PAEL experiment, except that the SSTA are the composites for AMO+/La Niña, AMO-/El Niño and AMO-/La Niña cases, respectively. Each experiment was integrated for 55 years and only the last 45 years of the integrations were used to avoid any influence of the initial conditions. The differences between each sensitivity experiment and CTRL ensemble means are regarded as the specific SSTA forcing effects.

3. Observed modulation of the ENSO-NAO relationship by the AMO

Figure 1 shows the time evolution of the DJF Niño3.4 and JMF NAO indices. Conspicuous interannual variability can be found in these two indices with a weak out-of-phase relationship between them (R=-0.15, nonsignificant at the 95% confidence level). Interestingly, the negative NAO phase usually corresponds to El Niño events during the positive AMO phase. Most La Niña events accompany the positive NAO phase during a negative AMO phase. In contrast, the NAO responses to El Niño events during the negative AMO phase and La Niña events during the positive AMO phase are inconsistent. It seems that the ENSO-NAO relationship is dependent upon the AMO phase.

We next categorize ENSO events into four types according to AMO phase: that is, El Niño events during a positive AMO phase (AMO+/El Niño) and El Niño events during a negative AMO phase (AMO-/El Niño), La Niña events during a positive AMO phase (AMO+/La Niña) and La Niña events during a negative AMO phase (AMO-/La Niña) (see Table 2). Figure 2 shows the composites of anomalous winter SLP and 850 hPa horizontal winds for these four cases over the North Atlantic region. Obviously negative and positive NAO-like atmospheric circulation patterns appear over the North Atlantic for the AMO+/El Niño and AMO-/La Niña composites respectively (Figure 2a and 2d), despite a slightly westward shift of the anomalous center relative to the conventional NAO pattern. Nonetheless, no obvious NAO-like atmospheric circulation anomalies can be observed over the North Atlantic for the

194 AMO-/El Niño and AMO+/La Niña composites (Figure 2b and 2c). It can be seen that
195 the NAO response is significantly strengthened (weakened) when ENSO and AMO
196 occur as in-phase (out-of-phase) combinations. This combined effect is further
197 examined for the AMO and ENSO based on the NCEP/NCAR 20CR reanalysis data
198 with its longer data period. Likewise, we can also observe significant (nonsignificant)
199 NAO-like atmospheric circulation patterns during ENSO and AMO in-phase
200 (out-of-phase) combinations (Figure 3).

201 The above analyses demonstrate that the AMO plays an important role in
202 permitting or denying the ENSO-NAO relationship. In order to clarify possible
203 mechanisms for different NAO responses to ENSO during different AMO phases, in
204 Figure 4 we present the regression of atmospheric circulation anomalies with respect
205 to both AMO and ENSO indices separately, to determine if there is any similarity. The
206 atmospheric circulation pattern regressed against the AMO index resembles the
207 typically negative NAO-like pattern (Figure 4a), consistent with previous studies (e.g.,
208 Kavvada et al. 2013; Peings and Magnusdottir 2014). Meanwhile, the regressed SLP
209 and wind anomalies against the Niño3.4 index also show similar negative NAO-like
210 features over the North Atlantic. In comparison, the ENSO-related atmospheric
211 anomalies north of 50°N are weaker and the negative NAO-like pattern cannot extend
212 further east toward the land. The ENSO-related NAO anomalies are supported by
213 experiments forced only by tropical Pacific SSTA of ENSO (Zhang et al. 2015, 2018).
214 The broadly analogous atmospheric responses to ENSO and the AMO over the North
215 Atlantic indicate a potential combined effect on NAO variability forced by ENSO and

the AMO. When ENSO and the AMO occur as in-phase combinations, the NAO-like atmospheric circulation pattern should be strong and prominent. However, if ENSO and the AMO occur as out-of-phase combinations (for example, La Niña during AMO+), the NAO responses are inconsistent, resulting from offsetting effects of each other.

4. Possible modulation mechanisms associated with the AMO

We now turn to explore possible mechanisms responsible for the AMO modulation effect on the ENSO-NAO relationship. Figure 5 shows the composite anomalies of JFM SST and 1000 hPa horizontal winds for the aforementioned four cases. The SSTA during El Niño under both positive and negative AMO phases has similar patterns in the tropical Pacific, exhibiting a warming in the eastern Pacific and cooling in the surrounding regions with basically the same intensities and center positions (Figure 5a and c). Similar conditions are shown for La Niña events with positive and negative AMO phases (Figure 5b and d). Therefore, the AMO modulation effect on the ENSO pattern and intensity seems ignorable and is not considered in this study. However, Figure 5 displays very different SSTAs in the North Pacific and in the tropical and North Atlantic. Considering the high background SST, the tropical SSTA can easily excite local convection anomalies, which thus gives rise to extra-tropical atmospheric anomalies and further ocean anomalies via the "atmospheric bridge" mechanism (e.g., Alexander et al. 2002). In contrast, SSTA in the mid-latitudes is usually passive in air-sea interaction processes (Neelin et al. 1987).

So, the tropical North Atlantic may be the key region for AMO modulation of the ENSO-associated atmospheric anomalies. Here, we define the area-averaged SSTA in the tropical North Atlantic region (5°N-25°N, 15°W-55°W) as the TNA index and in Figure 6 display the spatial pattern of the regressed SLP anomaly pattern onto this TNA index. We find a distinct north-south dipole of SLP anomalies with one center located near Iceland and the other of opposite sign spanning the central latitudes of the North Atlantic between 20°N and 40°N, resembling a negative NAO-like pattern. This result is consistent with many previous studies (e.g., Brönnimann, 2007a; Peng et al. 2002, 2005). A possible mechanism suggested by Li et al. (2007) is that the TNA SSTA could excite an anomalous heating over the tropical North Atlantic, which results in a Rossby wave train propagating northeastward. Then, this wave train leads to anomalous transient-eddy activity in the North Atlantic jet exit area. This anomalous transient-eddy forcing acts linearly on the time-mean flow with a NAO-like atmospheric pattern. Thus the relatively strong TNA SSTA that occurs during AMO+/El Niño and AMO-/La Niña combinations tends to favor strong NAO responses. However, the absence of TNA SSTA during AMO-/El Niño and AMO+/La Niña combinations leads to inconsistent responses of the NAO that are not robust.

The next scientific question that remains to be answered is how this different TNA SSTA is generated. Many previous studies have shown that the TNA SST tends to increase (decrease) after the peak of El Niño (La Niña) due to an atmospheric bridge between the tropical eastern Pacific and Atlantic Oceans (e.g., Enfied and Mayer 1997; Nicholson 1997; Wang 2002). Thus, the TNA SSTA is observed to lag

ENSO by several months. The regressed North Atlantic JFM SSTA against the DJF Niño3.4 index also confirmed this well-known ENSO-teleconnected effect (figure not shown). Simultaneously, the AMO is a basin-wide dominant SSTA mode in the North Atlantic on multidecadal time scales. Therefore, when the AMO and ENSO are in phase, these two SSTA act in superposition in TNA and thus the anomaly is robust with strong signal (Figure 7). For example, under the long-term warming background SST associated with the positive AMO phase, the El Niño-associated tropical Pacific SST warming further enhances the already warm TNA SSTA (Figure 5a). This strong TNA SSTA then leads to a prominent NAO response in the atmosphere. On the contrary, when AMO and ENSO are out of phase, these two opposite-sign responses in the TNA counteract each other, resulting in a nonsignificant TNA SSTA (Figure 8) and thus an unstable NAO response.

We further examine the effect of the AMO on the ENSO-NAO relationship based on HadCM3 historical simulations (146 years) derived from the Coupled Model Intercomparison Project phase 5 (CMIP5). These simulations provide more samples of the AMO in each phase, compared to the limited observational record. The model composites of simulated JFM SLP anomalies and TNA SSTA indices for the four different phase combinations of ENSO and AMO are shown in Figures 8 and 9, respectively. During the late winter of AMO+/El Niño combinations, the positive SSTA over the TNA region is robust (Figure 9), which corresponds to significant negative NAO responses (Figure 8a). The simulated responses during AMO-/La Niña combinations in late winter are generally the opposite (Figure 8d and 9). However,

neither the TNA SSTA nor the atmospheric circulation responses over the North Atlantic are obvious when the AMO and ENSO occur in out-of-phase combinations (Figure 8b-c and 9).

Finally, the combined influences of ENSO and the AMO on the NAO are confirmed by GFDL AM2.1 atmosphere-only experiments. Figure 10 shows the simulated anomalous SLP responses to the different SSTA combinations of the AMO and ENSO. It is found that obvious negative and positive NAO-like atmospheric circulation patterns appear over the North Atlantic for the PALA and NALA experiments, respectively (Figure 10a and 10d). Nevertheless, no obvious NAO-like atmospheric circulation anomalies can be simulated in the NAEL and PALA experiments (Figure 10b and 10c). These results also suggest a strong AMO modulation effect on the ENSO-NAO relationship via the TNA SSTA. The consistency between observations and model simulations increase our confidence in the aforementioned mechanism responsible for modulation of the ENSO-NAO relationship by the AMO.

5. Summary and discussion

A general physical link has been detected between ENSO and the NAO in late winter, but with a high uncertainty. In this study we demonstrate that the uncertainty of the ENSO-NAO relationship is partly due to decadal modulation by the AMO, which is therefore of importance for seasonal-to-interannual prediction of the NAO. To illustrate this AMO modulation, we categorize ENSO events into four groups

304 according to AMO phase: AMO+/El Niño, AMO-/El Niño, AMO+/La Niña and
305 AMO-/La Niña. It is found that when the ENSO and AMO occur as in-phase
306 combinations (i.e., AMO+/El Niño and AMO-/La Niña), then El Niño (La Niña)
307 events frequently correspond to significantly negative (positive) NAO-like
308 atmospheric anomalies; this gives a significant negative ENSO-NAO relationship in
309 late winter. In contrast, there are no significant atmospheric anomalies over the North
310 Atlantic when ENSO and the AMO occur as out-of-phase combinations (i.e.,
311 AMO-/El Niño and AMO+/La Niña).

312 The tropical North Atlantic (TNA) SSTA is proposed to serve as an important
313 medium for AMO modulation of the ENSO-NAO relationship, since it can excite
314 remarkable NAO-like atmospheric circulation anomalies. The TNA SSTA responses
315 to ENSO and the AMO are broadly analogous. When AMO and ENSO are in phase,
316 their influences on the TNA SSTA occur in superposition and thus the strong TNA
317 SSTA favors a significant NAO-associated atmospheric response. On the other hand,
318 when AMO and ENSO are out of phase, the TNA SSTA responses counteract each
319 other and thus the response is very weak. As a summary, a schematic (Figure 11) for
320 the combined impacts on the NAO exerted by ENSO and the AMO is provided.

321 We have also checked possible effects of another prominent decadal mode in the
322 North Pacific (i.e., the Pacific Decadal Oscillation or PDO). Almost no remarkable
323 impacts of the PDO on the ENSO-NAO relation can be detected (not shown). In the
324 present study, we thus emphasize the clear modulation of the ENSO-NAO
325 relationship by the AMO. We acknowledge that many factors other than the TNA

SSTA, such as volcanic eruptions (Shindell et al. 2004; Driscoll et al. 2012), Arctic sea ice (Hilmel and Jung 2000; Seierstad and Bader 2009) and internal atmospheric variability (Kumar and Hoerling 1998), may also impact the NAO-related atmospheric circulation. In addition, ENSO itself exhibits a considerable degree of diversity in its SSTA pattern, which also complicates its connection with the NAO (e.g., Greatbatch et al. 2004; Graf and Zanchettin 2012; Zhang et al. 2015, 2018). All these factors may increase the uncertainty of the ENSO-NAO relationship.

Acknowledgements

This work was supported by the National Nature Science Foundation of China (41675073), the SOA Program on Global Change and Air-Sea interactions (GASI-IPOVAI-03). AGT was supported by the NCAS-Climate Core Agreement, Contract number R8/H12/83/00.

340 **REFERENCES**

341 Alexander, L. V., X. Zhang, T. C. Peterson, J. Caesar, and B. Gleason, 2006: Global
342 observed changes in daily climate extremes of temperature and precipitation. *J.*
343 *Geophys. Res.*, **111**, D05109.

344 Alexander, M. A., I. Blade, M. Newman, J. R. Lanzante, N.-C. Lau and J. D. Scott
345 2002: The atmospheric bridge: The influence of ENSO teleconnections on
346 air-sea interaction over the global oceans, *J. Clim.*, **15**, 2205-2231.

347 Bell, C. J., L. J. Gray, A. J. Charlton-Perez, M. M. Joshi, and A. A. Scaife, 2009:
348 Stratospheric communication of El Niño teleconnections to European winter. *J.*
349 *Clim.*, **22**, 4083-4096.

350 Brönnimann, S., 2007a: Impact of El Niño-Southern Oscillation on European, *climate.*
351 *Rev. Geophys.*, **45**, RG3003.

352 ——, E. Xoplaki, C. Casty, A. Pauling, and J. Luterbacher, 2007b: ENSO influence
353 on Europe during the last centuries. *Clim. Dyn.*, **28**, 181-197.

354 Castanheira, J. M., and H. F. Graf, 2003: North Pacific-North Atlantic relationships
355 under stratospheric control? *J. Geophys. Res.*, **108**, 4036,
356 doi:10.1029/2002JD002754.

357 Cattiaux, J., R. Vautard, C. Cassou, P. Yiou, V. Masson-Delmotte, and F.
358 Codron, 2010: Winter 2010 in Europe: A cold extreme in a warming
359 climate. *Geophys. Res. Lett.,* **37**, L20704.

360 Cohen, J. L., J. C. Furtado, M. A. Barlow, V. A. Alexeev, and J. E. Cherry, 2012:
361 Arctic warming, increasing snow cover and widespread boreal winter cooling.
362 *Environ. Res. Lett.*, **7**, 011004.

363 Compo, G. P., J. S. Whitaker, P. D. Sardeshmukh, N. Matsui, and R. J. Allan, 2011: .
364 *Quarterly J. Roy. Meteorol. Soc.*, **137**, 1-28.

365 Davini, P., J. Hardenberg, and S. Corti, 2015: Tropical origin for the impacts of the
366 Atlantic Multidecadal Variability on the Euro-Atlantic climate. *Environ. Res.*
367 *Lett.*, **10**, 094010.

368 Deser, C., and H. Teng, 2008: Evolution of Arctic sea ice concentration trends and the

role of atmospheric circulation forcing, 1979-2007. *Geophys. Res. Lett.*, **35**, L02504.

Dong, B. W., R. T. Sutton and A. A. Scaife, 2006: Multidecadal modulation of El Niño-Southern Oscillation (ENSO) variance by Atlantic Ocean sea surface temperatures. *Geophys. Res. Lett.*, **33**, L08705.

Driscoll, S., A. Bozzo, L. G. Gray, A. Robock, and G. Stenchikov 2012: Coupled Model Intercomparison Project 5 (CMIP5) simulations of climate following volcanic eruptions. *J. Geophys. Res.*, **117**, 127-135.

Drouard. M., G. Riviere, and P. Arbogast, 2015: The link between the North Pacific climate variability and the North Atlantic Oscillation via downstream propagation of synoptic waves. *J. Clim.*, **28**, 3957-3976.

Dunstone, N., D. Smith, A. Scaife, L. Hermanson, R. Eade, N. Robinson, M. Andrews, and J. Knight, 2016: Skilful predictions of the winter North Atlantic Oscillation one year ahead. *Nat. Geosci.*, **9**, 809-814.

Enfield, D. B., A. M. Mestas-Nuñez, and P. J. Trimble, 2001: The Atlantic multidecadal oscillation and its relation to rainfall and river flows in the continental US. *Geophys. Res. Lett.*, **28**, 2077-2080.

——, and D. A. Mayer, 1997: Tropical Atlantic sea surface temperature variability and its relation to El Niño-Southern Oscillation. *J. Geophys. Res.*, **102**, 929-945.

Fraedrich, K., and K. Muller, 1992: Climate anomalies in Europe associated with ENSO extremes. *Int. J. Climatol.*, **12**, 25-31.

——, 1994: An ENSO impact on Europe? Tellus, **46A**, 541-552.

Geng, X., W. J. Zhang., M. F. Stuecker, and F. F. Jin, 2017: Strong sub-seasonal wintertime cooling over East Asia and Northern Europe associated with super El Niño events. *Sci. Rep.*, **7**, doi: 10.1038/s41598-017-03977-2.

Gouirand, I., and V. Moron, 2003: Variability of the impact of El Niño-Southern Oscillation on sea-level pressure anomalies over the North Atlantic in January to March (1874-1996). *Int. J. Climatol.*, **23**, 1549-1566.

Graf, H. F., and D. Zanchettin, 2012: Central Pacific El Niño, the"subtropical bridge", and Eurasian climate. *J. Geophys. Res.*, **117**, D01102.

399 Greatbatch, R. J., J. Lu, and K. A. Peterson, 2004: Nonstationary impact of ENSO on
400 Euro-Atlantic winter climate. *Geophys. Res. Lett.*, **31**, L02208.
401 Groisman, P. Y., and E. Y. Rankova, 2001: Precipitation trends over the Russian
402 permafrost-free zone: Removing the artifacts of pre-processing. *Int. J. Climatol.*,
403 **21**, 657-678.
404 ——, R. W. Knight, D. R. Easterling, T. R. Karl, G. C. Hegerl, and V. N. Razuvaev
405 2005: Trends in intense precipitation in the climate record. *J. Clim.*, **18**,
406 1326-1350.
407 Hilmel, M., and T. Jung, 2000: Evidence for a recent change in the link between the
408 North Atlantic Oscillation and Arctic sea ice export. *Geosphy. Res. Lett.*, **27**,
409 989-992.
410 Hurrell, J. W., 1995: Decadal trends in the North-Atlantic oscillationregional
411 temperatures and precipitation. Science, **269**, 676-679.
412 ——, 1996: Influence of variations in extratropical wintertime teleconnections on
413 Northern Hemisphere temperature. *Geophys. Res. Lett.*, **23**, 665-668.
414 ——, Y. Kushnir, G. Ottersen, and M. Visbeck, 2003: An overview of the North
415 Atlantic Oscillation. In: Hurrell, J. W., Y. Kushnir, G. Ottersen, and M. Visbeck,
416 (eds) The North Atlantic Oscillation: climate significance and environmental
417 impact. American Geophysical Union, Washington, pp 1-35.
418 Ineson, S., and A. A. Scaife, 2009: The role of the stratosphere in the European
419 climate response to El Niño. *Nat. Geosci.*, **2**, 32-36.
420 Infanti, J. M., and B. P. Kirtman, 2016: North American rainfall and temperature
421 prediction response to the diversity of ENSO. *Clim. Dyn.*, **46**, 3007-3023.
422 Johansson, A., 2007: Prediction Skill of the NAO and PNA from Daily to Seasonal
423 Time Scales. *J. Clim*., **20**, 1957-1975.
424 Kalnay, E., M. Kanamitsu, R. Kistler, and W. Collins, 1996: The NCEP/NCAR
425 40-year reanalysis project. *Bull. Am. Meteorol. Soc.*, **77**, 437-471.
426 Kavvada, A., A. Ruiz-Barradas, and S. Nigam, 2013: AMO's structure and climate
427 footprint in observations and IPCC AR5 climate simulations. *Clim. Dyn.*, **41**,
428 1345-1364.

Kerr, R. A., 2000: A North Atlantic climate pacemaker for the centuries. Science, **288**, 1984-1986.

Klein, S. A., B. J. Soden, and N. -C. Lau, 1999: Remote sea surface temperature variations during ENSO: Evidence for a tropical atmospheric bridge. *J. Clim.*, **12**, 917-932.

Kumar, A., and M. P. Hoerling, 1998: Annual cycle of Pacific/North American seasonal predictability associated with different phases of ENSO. *J. Clim.*, **11**, 3295-3308.

Lau, N. -C., and M. J. Nath, 2003: Atmosphere-ocean variations in the Indo-Pacific sector during ENSO episodes. *J. Clim.*, **16**, 3-20.

Li, J. P., and J. X. L. Wang, 2003: A new North Atlantic Oscillation index and its variability. *Adv. Atmos. Sci.*, **20**, 661-676.

——, C. Sun, and F. F. Jin, 2013: NAO implicated as a predictor of Northern Hemisphere mean temperature multidecadal variability. *Geophys. Res. Lett.*, **40**, 5497-5502.

——, and C. Q. Ruan, 2018: The North Atlantic-Eurasian teleconnection in summer and its effects on Eurasian climates. *Environ. Res. Lett.*, **13**, 024007.

Li., S. L., W. A. Robinson, M. P. Hoerling, and K. M. Weickmann, 2007: Dynamics of the extratropical response to a tropical Atlantic SST anomaly. *J. Clim.*, **20**, 560-574.

Li, Y., and N. -C. Lau, 2012a: Impact of ENSO in the atmospheric variability over the North Atlantic in late winter-role of transient eddies. *J. Clim.*, **25**, 320-342.

——, and N. -C. Lau, 2012b: Contributions of downstream eddy development to the teleconnection between ENSO and the atmospheric circulation over the North Atlantic. *J. Clim.*, **25**, 4993-5010.

Lu, R. Y., B. W. Dong and H. Ding, 2006: Impact of the Atlantic Multidecadal Oscillation on the Asian summer monsoon. *Geophys. Res. Lett.*, **33**, L24701.

Mathieu, P. P., R. T. Sutton, B. W. Dong, and M. Collins, 2004: Predictability of winter climate over the North Atlantic European region during ENSO events. *J. Clim.*, **17**, 1953-1974.

459 Moron, M. and G. Plaut, 2003: The impact of El Niño Southern Oscillation upon
460 weather regimes over Europe and the North Atlantic boreal winter. *Int. J.*
461 *Climatol.*, **23**, 363-379.
462 Moron, V. and I. Gouirand, 2003: Seasonal modulation of the El Niño Southern
463 Oscillation relationship with sea level pressure anomalies over the North Atlantic
464 in October-March 1873-1996. *Int. J. Climatol.*, **23**, 143-155.
465 Msadek, R., C. Frankignoul, and L. Li, 2011: Mechanisms of the atmospheric
466 response to North Atlantic multidecadal variability: a model study. *Clim. Dyn.*,
467 **36**, 1255-1276.
468 Neelin, J. D., I. M. Held and K. H. Cook, 1987: Evaporation-wind feedback and
469 low-frequency variability in the tropical atmosphere. *J. Atmos. Sci.*, **44**,
470 2341-2348.
471 Nicholson, S. E., 1997: An analysis of the ENSO signal in the Tropical Atlantic and
472 Western Indian Ocean. *Int. J. Climatol.*, **17**, 345-375.
473 Omrani, N. E., N. S. Keenlyside, J. Bader, and E. Manzini, 2014: Stratosphere key for
474 wintertime atmospheric response to warm Atlantic decadal conditions. *Clim.*
475 *Dyn.*, **42**, 649-663.
476 Peings, Y., and G. Magnusdottir, 2014: Forcing of the wintertime atmospheric
477 circulation by the multidecadal fluctuations of the North Atlantic Ocean. *Environ.*
478 *Res. Lett.*, **9**, 034018.
479 Peng, S. L., W. A. Robinson, and S. L. Li, 2002: North Atlantic SST forcing of the
480 NAO and relationships with intrinsic hemispheric variability. *Geophys. Res. Lett.*,
481 **29**, doi:10.1029/2001GL014043.
482 ——, ——, ——, and M. P. Hoerling, 2005 Tropical Atlantic SST Forcing of
483 Coupled North Atlantic Seasonal Responses. *J. Clim.*, **18**, 480-496.
484 Robertson, A. W., and C. R. Mechoso, and Y. J. Kim, 2000: The influence of the
485 Atlantic sea surface temperature anomalies on the North Atlantic Oscillation. *J.*
486 *Clim.*, **13**, 122-138.
487 Ropelewski, C. F., and M. S. Halpert, 1987: Global and regional scale precipitation
488 patterns associated with the El Niño/Southern Oscillation. *Mon. Weather Rev.*,

115, 1606-1626.

Scaife, A. A., C. K. Folland, L. V. Alexander, A. Moberg, and J. R. Knight, 2008: European climate extremes and the North Atlantic Oscillation. *J. Clim.*, **21** 72-83.

Seierstad, I. A., and J. Bader, 2009: Impact of a projected future Arctic Sea Ice reduction on extratropical storminess and the NAO. *Clim. Dyn.*, **33**, 937-943.

Shindell, D. T., G. A. Schmidt, M. E. Mann, and G. Faluvegi 2004: Dynamic winter climate response to large tropical volcanic eruptions since 1600. *J. Geophys. Res.*, **109**, D05104.

Smith, D. M., A. A., Scaife, R. Eade, and J. R. Knight, 2016: Seasonal to decadal prediction of the winter North Atlantic Oscillation: emerging capability and future prospects. *Q. J. R. Meteorol. Soc.*, **142**, 611-617.

Smith, T. M., R. W. Reynolds, T. C. Peterson, and J. Lawrimore, 2008: Improvements to NOAA's historical merged land-ocean surface temperature analysis (1880-2006). *J. Clim.*, **21**, 2283-2296.

Stenchikov, G., K. Hamilton, R. J. Stouffer, A. Robock, V. Ramaswamy, B. Santer, and H. F. Graf, 2006: Arctic Oscillation response to volcanic eruptions in the IPCC AR4 climate models. *J. Geophys. Res.*, **111**, D07107.

Sun, Y. B., S. C. Clemens, C. Morrill, X. Lin, X. Wang, and Z. An, 2011: Influence of Atlantic meridional overturning circulation on the East Asian winter monsoon. *Nat. Geosci.*, **5**, 46-49.

Sun, C., J. P. Li, and F. F. Jin, 2015: A delayed oscillator model for the quasiperiodic multidecadal variability of the NAO. *Clim. Dyn.*, **45**, 2083-2099.

Sutton, R. T., B. Dong, 2012: Atlantic Ocean influence on a shift in European climate in the 1990s. *Nat. Geosci.*, **5**, 788-792.

——, and D. L. R. Hodson, 2005: Atlantic Ocean forcing of North American and European summer climate. *Science*, **309**, 115-118.

Taylor, K. E., R. J. Stouffer, and G. A. Meehl, 2012: An Overview of CMIP5 and the Experiment Design. *Bull. Amer. Meteor. Soc.*, **93**, 485-498.

The GFDL Global Atmospheric Model Development Team, 2004: The New GFDL

519 Global Atmosphere and Land Model AM2-LM2: evaluation with prescribed SST
520 simulations. *J. Clim.*, **17**, 4641-4673.
521 Thompson, D. W. J., and J. M. Wallace, 2000: Annular modes in the extratropical
522 circulation. Part I: month-to-month variability. *J. Clim.*, **13**, 1000-1016.
523 Ting, M. F., Y. Kushnir, R. Seager, and C. H. Li, 2011: Robust features of Atlantic
524 multi-decadal variability and its climate impacts. *Geophys. Res. Lett.*, **38**,
525 L17705.
526 ——, Y. Kushnir, and C. H. Li, 2014: North Atlantic Multidecadal SST Oscillation:
527 External forcing versus internal variabilit. *J. Mar. Sys.*, **133**, 27-38.
528 Toniazzo, T., and A. A. Scaife, 2006: The influence of ENSO on winter North Atlantic
529 climate. *Geophys. Res. Lett.*, **33**, L24704.
530 Wang, C. Z., 2002: Atlantic climate variability and its associated atmospheric
531 circulation cells. *J. Clim.*, **15**, 1516-1536.
532 ——, and J. Picaut, 2004: Understanding ENSO physics-A review, in Earth's Climate:
533 The Ocean-Atmosphere Interaction. *Geophys. Monogr. Ser.*, **147**, 21-48.
534 ——, H. Liu, and S. -K. Lee, 2010: The record-breaking cold temperatures during the
535 winter of 2009/2010 in the Northern Hemisphere. *Atmos. Sci. Lett.*, **11**, 161-168.
536 Watanabe, M., and M. Kimoto, 1999: Tropical-extratropical connection in the
537 Atlantic atmosphere-ocean variability. *Geophys. Res. Lett.*, **26**, 2247-2250.
538 Wettstein, J. J., and L. O. Mearns, 2002: The influence of the North Atlantic-Arctic
539 Oscillation on mean, variance, and extremes of temperature in the northeastern
540 United States and Canada. *J. Clim.*, **15**, 3586-3600.
541 Wu. A., and W. W. Hsieh, 2004: The nonlinear association between ENSO and the
542 Euro-Atlantic winter sea level pressure. *Clim. Dyn.*, **23**, 859-868.
543 Zhang, R., T. L. Delworth, and I. M. Held, 2007: Can the Atlantic Ocean drive the
544 observed multidecadal variability in Northern Hemisphere mean temperature?
545 *Geophys. Res. Lett.*, **34**, L02709.
546 Zhang, W. J., L. Wang, B. Q. Xiang, L. Qi and J. H. He, 2015a: Impacts of two types
547 of La Niña on the NAO during boreal winter. *Clim. Dyn.*, **44**, 1351-1366.
548 ——, Z. Q. Wang, M. F. Stuecker, A. G. Turner, F. F. Jin, and X. Geng, 2018: Impact

549 of ENSO longitudinal position on teleconnections to the NAO. *Clim. Dyn.*,
550 http://doi.org/10.1007/s00382-018- 4135-1.
551

552 **Table 1**. El Niño and La Niña events for the 1950-2016 period based on the Niño3.4

553 index.

El Niño events	La Niña events
1953/54, 1957/58, 1963/64, 1965/66, 1968/69, 1969/70, 1972/73, 1976/77, 1977/78, 1982/83, 1986/87, 1987/88, 1991/92, 1994/95, 1997/98, 2002/03, 2004/05, 2006/07, 2009/10, 2015/16	1950/51, 1954/55, 1955/56, 1962/63, 1964/65, 1967/68, 1970/71, 1971/72, 1973/74, 1974/75, 1975/76, 1984/85, 1988/89, 1995/96, 1998/999, 1999/00, 2000/01, 2005/06, 2007/08, 2008/09, 2010/11, 2011/2012, 2012/2013, 2013/2014

554

555 **Table 2**. List of the conducted SST perturbation experiment

Experiment	Description of the SST perturbation
PAEL	Composite SST anomalies for the AMO+/El Niño case are imposed on the monthly climatological SST from December to March in the tropical Pacific (30°S-30°N, 120°E-90°W) and the tropical North Atlantic (0-30°N, 80°W-0) regions.
NAEL	As in PAEL but the composite SST anomalies for the AMO-/El Niño case are imposed.
PALA	As in PAEL but the composite SST anomalies for the AMO+/La Niña case are imposed.
NALA	As in PAEL but the composite SST anomalies for the AMO-/La Niña case are imposed.

556

557 **Table 3**. Category of El Niño and La Niña events for the 1950-2016 period according

558 to AMO phase.

Categories	Years
AMO+/El Niño	1953/54, 1957/58, 1963/64, 1965/66, 1997/98, 2002/03, 2004/05, 2006/07, 2009/10, 2015/16
AMO-/El Niño	1968/69, 1969/70, 1972/73, 1976/77, 1977/78, 1982/83, 1986/87, 1987/88, 1991/92, 1994/95
AMO+/La Niña	1950/51, 1954/55, 1955/56, 1962/63, 1964/65, 1998/999, 1999/00, 2000/01, 2005/06, 2007/08, 2008/09, 2010/11, 2011/2012, 2012/2013, 2013/2014
AMO-/La Niña	1967/68, 1970/71, 1971/72, 1973/74, 1974/75, 1975/76, 1984/85, 1988/89, 1995/96

559

560 **Figure Captions**

561 Figure 1. Time evolution of JFM NAO (blue solid line), DJF Niño3.4 (red dashed line)
562 and DJF AMO (bar) indices from 1950/51 to 2015/16 winter. Orange and green
563 dots represent the El Niño and La Niña winters, respectively. The decadal
564 component of AMO index is shown here, which is calculated using a 10-year
565 low-pass filter.

566 Figure 2. Composites of anomalous SLP (contours in hPa, from -4.0 to 3.0 by 1.0) and
567 850 hPa horizontal winds (vector in m/s) for (a) AMO+/El Niño; (b) AMO+/La
568 Niña; (c) AMO-/El Niño; (d) AMO-/La Niña cases based on NCEP/NCAR
569 reanalysis data. Shading represents those SLP anomalies above the 90%, 95%
570 and 99% confidence levels, respectively. The wind anomalies are only displayed
571 when the zonal or meridional wind anomalies are significant at the 90%
572 confidence level.

573 Figure 3. As in Figure 2, but for composites based on 20CR data in the period of
574 1900-2012 (contour in hPa, from -3.0 to 3.0 by 1.0).

575 Figure 4. Regressed anomalous patterns of SLP (contour in hPa, from -0.8 to 1.6 by
576 0.4) and 850 hPa horizontal winds (vector in m/s) with respect to the (a) AMO
577 and (b) Niño3.4 indices. Shading represents those SLP anomalies significant
578 above the 90%, 95% and 99% confidence levels, respectively. The wind
579 anomalies are shown only when the zonal or meridional wind anomalies are
580 significant at the 90% confidence level.

581 Figure 5. Composites of anomalous SST (shading in °C) and 1000 hPa horizontal

582 wind (vector in m/s) for the (a) AMO+/El Niño, (b) AMO+/La Niña, (c)
583 AMO-/El Niño, (d) AMO-/La Niña cases. Shading represents those SST
584 anomalies significant above the 90%, 95% and 99% confidence levels,
585 respectively. The wind anomalies are only displayed when the zonal or
586 meridional wind anomalies are significant at the 90% confidence level. The
587 yellow box (15°W-55°W, 5°N-25°N) is the domain used to define the tropical
588 North Atlantic (TNA) index.

589 Figure 6. Regressed anomalous patterns of JFM SLP (contour in hPa, from -1.6 to 3.2
590 by 0.8) with respect to the simultaneous TNA index. Shading represents those
591 SLP anomalies significant above the 90%, 95% and 99% confidence levels,
592 respectively. The yellow box is the domain used to define the tropical North
593 Atlantic (TNA) index.

594 Figure 7. Composites of tropical North Atlantic (TNA) indices for AMO+/El Niño,
595 AMO+/La Niña, AMO-/El Niño, and AMO-/La Niña cases. The error bars
596 represent one standard deviation error estimates.

597 Figure 8. As in Figure 2, but for composites based on the HadCM3 historical
598 simulations (contour in hPa, from -3.0 to 1.0 by 0.5).

599 Figure 9. As in Figure 7, but for composites based on the HadCM3 historical
600 simulations.

601 Figure 10. AM2.1 simulated JFM anomalous SLP (contour in hPa, from -4.0 to 5.0 by
602 1.0) responses to (a) PAEL, (b) PALA, (c) NAEL and (d) NALA SSTA forcings.
603 Shading represents those SLP anomalies significant above the 90%, 95% and 99%

confidence levels, respectively.

Figure 11. Schematic for AMO modulation of the ENSO-NAO relationship. "+" and "-" indicates the positive and negative phase, respectively. For instance, ENSO+ and ENSO- represent the positive ENSO phase (i.e., El Niño) and the negative ENSO phase (i.e., La Niña).

610 **List of Figures**

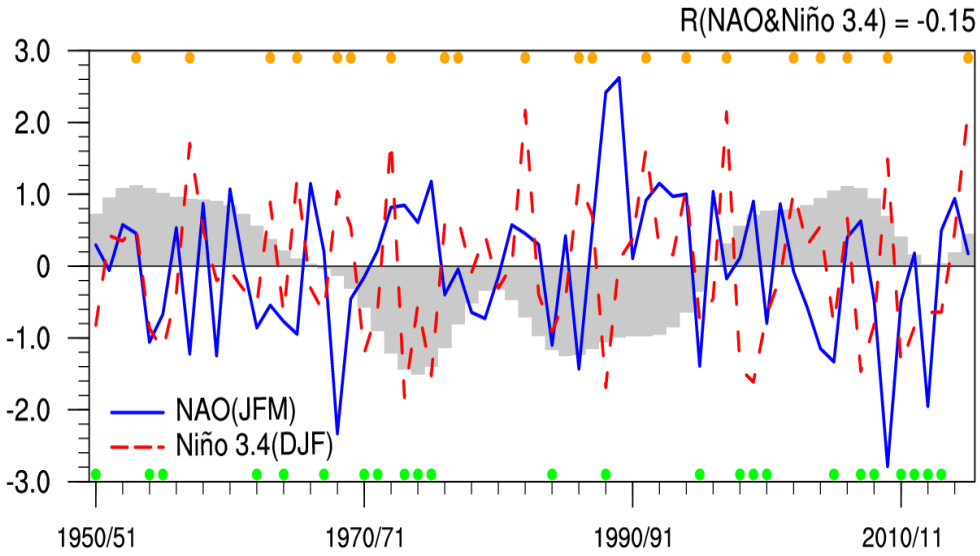

611

612 Figure 1. Time evolution of JFM NAO (blue solid line), DJF Niño3.4 (red dashed line)

613 and DJF AMO (bar) indices from 1950/51 to 2015/16 winter. Orange and green dots

614 represent the El Niño and La Niña winters, respectively. The decadal component of

615 AMO index is shown here, which is calculated using a 10-year low-pass filter.

616

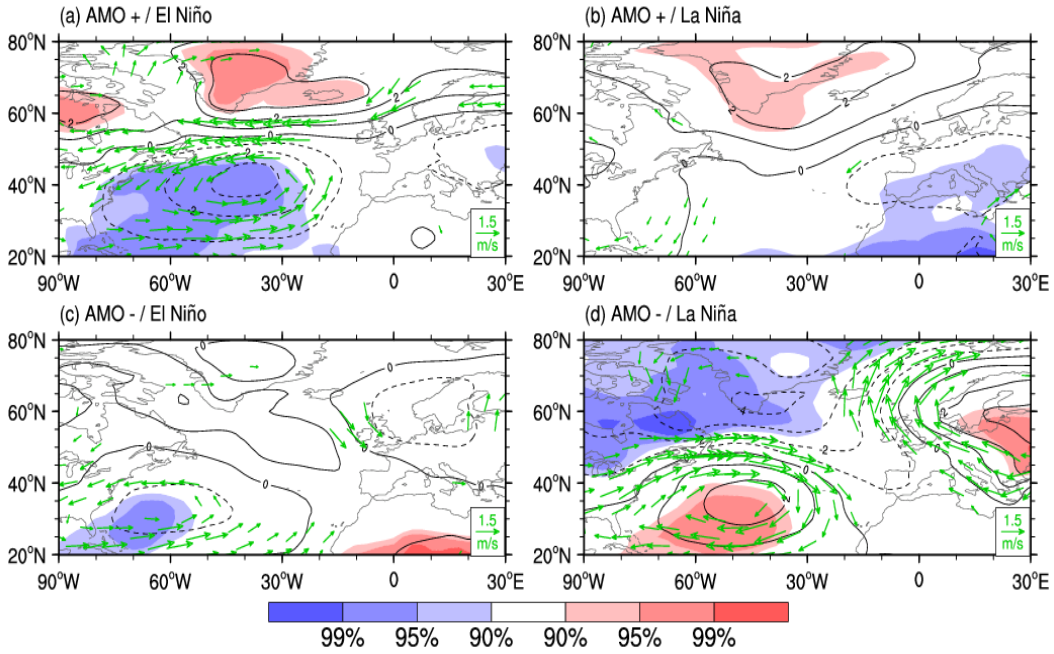

617

618 Figure 2. Composites of anomalous SLP (contours in hPa, from -4.0 to 3.0 by 1.0) and
619 850 hPa horizontal winds (vector in m/s) for (a) AMO+/El Niño; (b) AMO+/La Niña;
620 (c) AMO-/El Niño; (d) AMO-/La Niña cases based on NCEP/NCAR reanalysis data.
621 Shading represents those SLP anomalies significant above the 90%, 95% and 99%
622 confidence levels, respectively. The wind anomalies are only displayed when the
623 zonal or meridional wind anomalies are significant at the 90% confidence level.

624

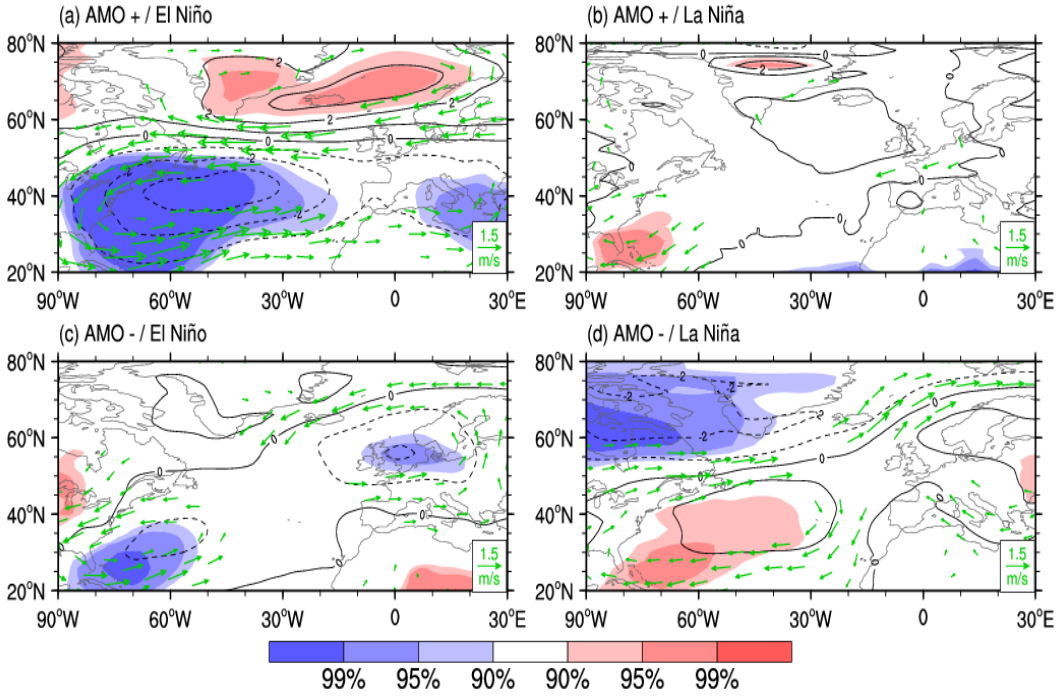

625

626 Figure 3. As in Figure 2, but for composites based on 20CR data in the period of

627 1900-2012 (contour in hPa, from -3.0 to 3.0 by 1.0).

628

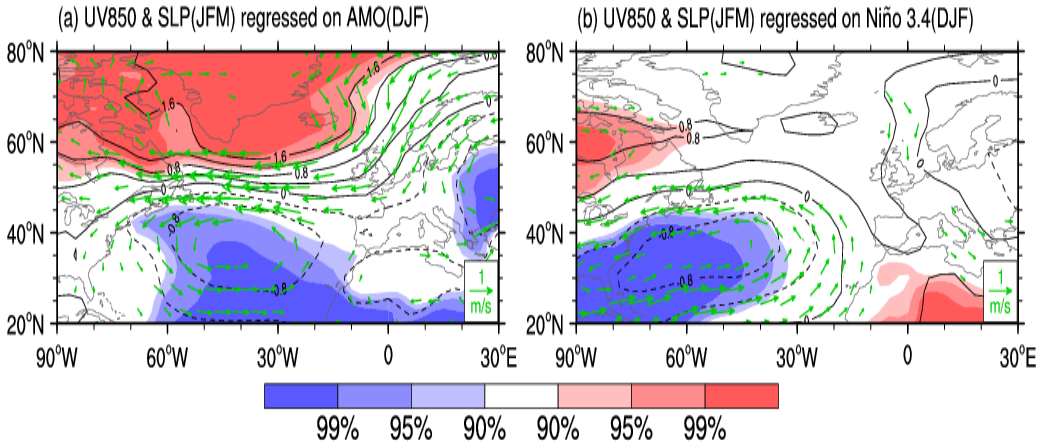

629

630 Figure 4. Regressed anomalous patterns of SLP (contour in hPa, from -0.8 to 1.6 by
631 0.4) and 850 hPa horizontal winds (vector in m/s) with respect to the (a) AMO and (b)
632 Niño3.4 indices. Shading represents those SLP anomalies significant above the 90%,
633 95% and 99% confidence levels, respectively. The wind anomalies are shown only
634 when the zonal or meridional wind anomalies are significant at the 90% confidence
635 level.

636

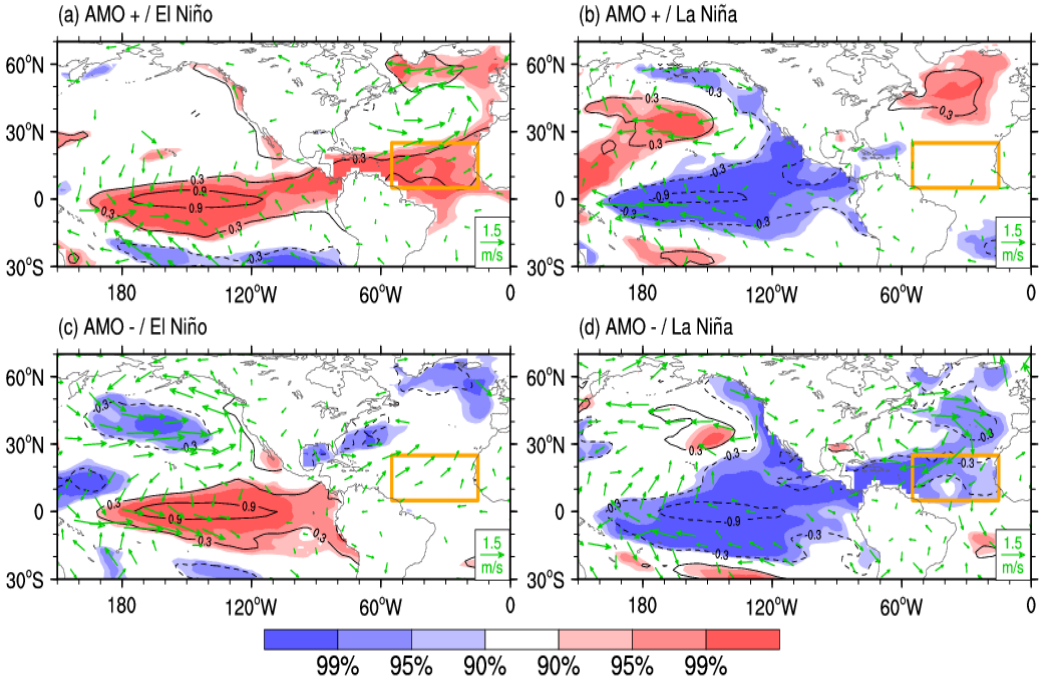

637

638 Figure 5. Composites of anomalous SST (shading in °C) and 1000 hPa horizontal
639 wind (vector in m/s) for the (a) AMO+/El Niño, (b) AMO+/La Niña, (c) AMO-/El
640 Niño, (d) AMO-/La Niña cases. Shading represents those SST anomalies significant
641 above the 90%, 95% and 99% confidence levels, respectively. The wind anomalies are
642 only displayed when the zonal or meridional wind anomalies are significant at the 90%
643 confidence level. The yellow box (15°W-55°W, 5°N-25°N) is the domain used to
644 define the tropical North Atlantic (TNA) index.

645

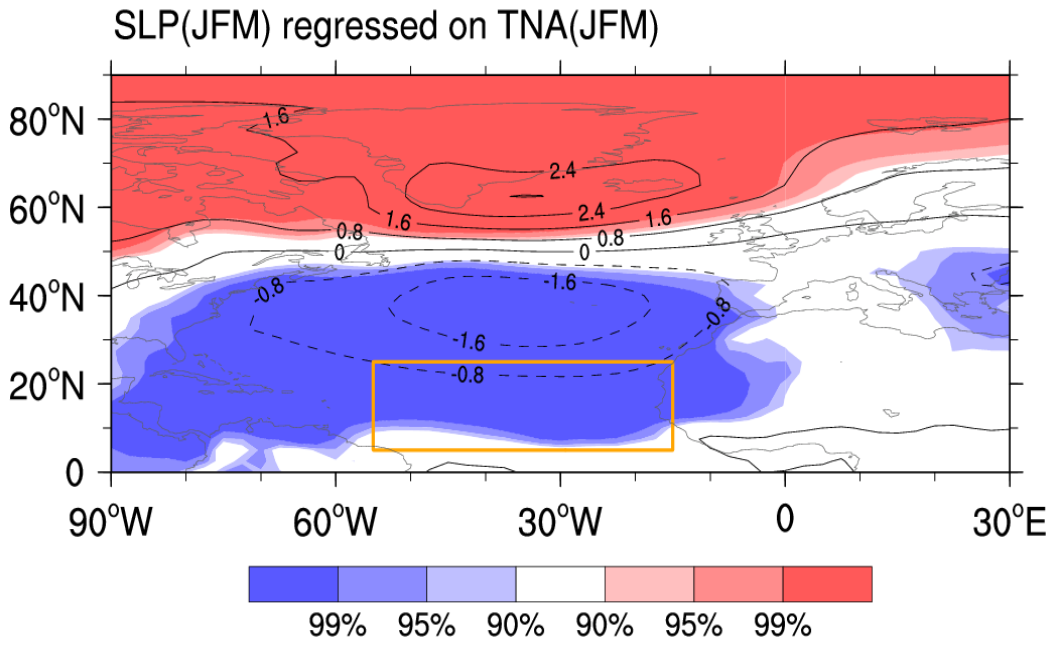

Figure 6. Regressed anomalous patterns of JFM SLP (contour in hPa, from -1.6 to 3.2 by 0.8) with respect to the simultaneous TNA index. Shading represents those SLP anomalies significant above the 90%, 95% and 99% confidence levels, respectively. The yellow box is the domain used to define the tropical North Atlantic (TNA) index.

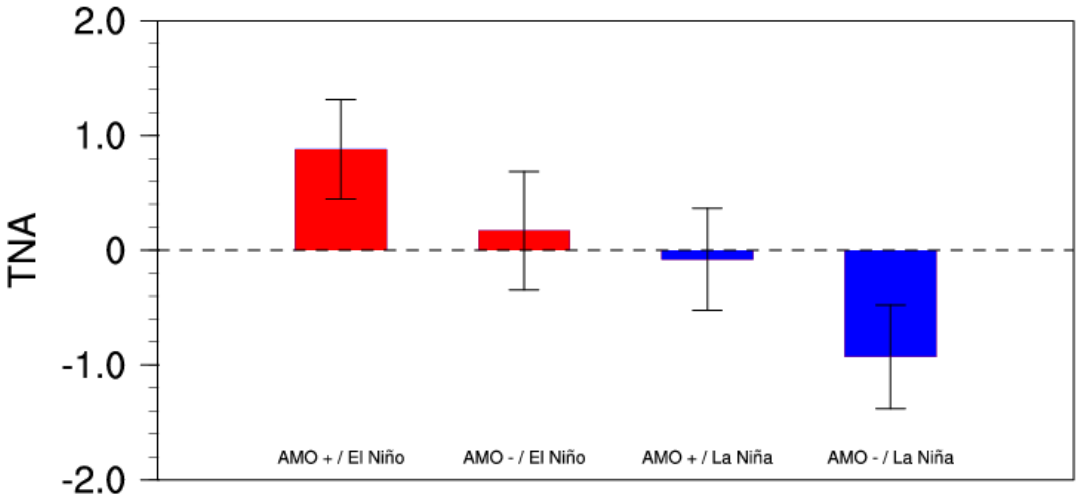

652

653 Figure 7. Composites of tropical North Atlantic (TNA) indices for the AMO+/El Niño,

654 AMO+/La Niña, AMO-/El Niño, AMO-/La Niña cases. The error bars represent one

655 standard deviation error estimates.

656

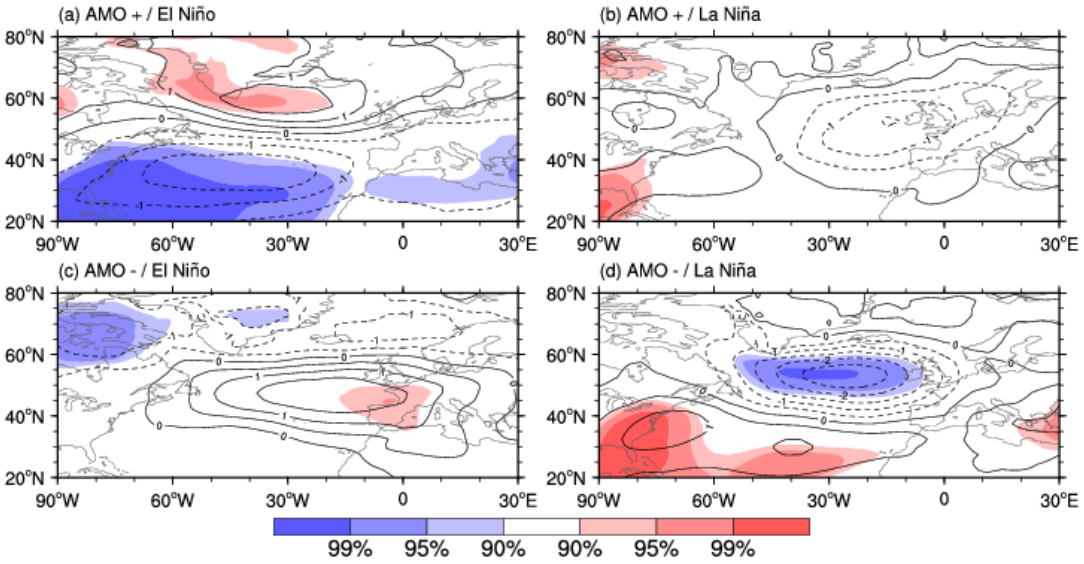

657

658 Figure 8. As in Figure 2, but for composites based on the HadCM3 historical

659 simulations (contour in hPa, from -3.0 to 1.0 by 0.5).

660

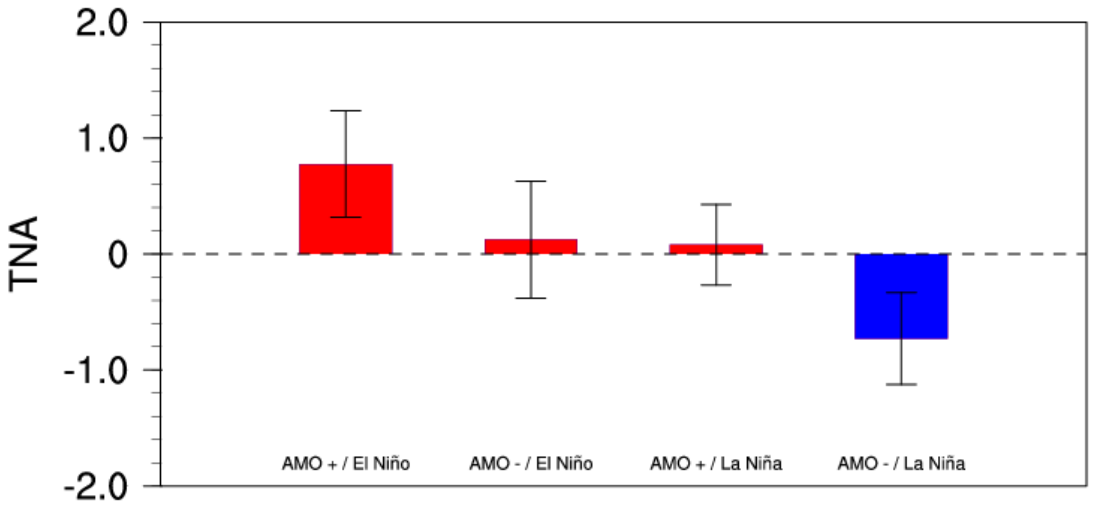

661

662 Figure 9. As in Figure 7, but for composites based on the HadCM3 historical

663 simulations.

664

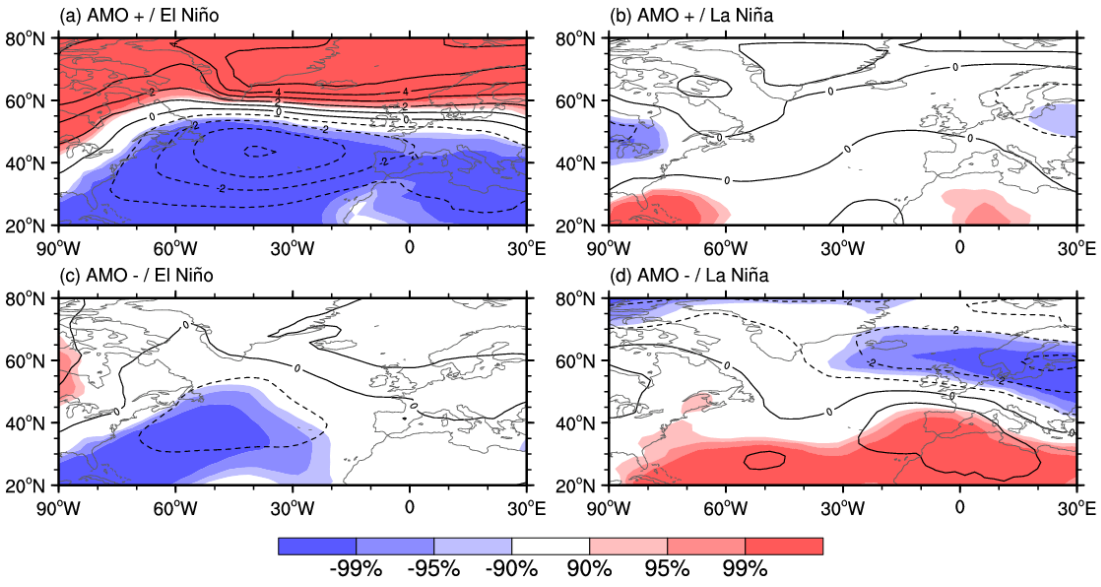

665

666 Figure 10. AM2.1 simulated JFM SLP responses (contour in hPa, from -4.0 to 5.0 by

667 1.0) to (a) PAEL, (b) PALA, (c) NAEL and (d) NALA SSTA forcings. Shading

668 represents those SLP anomalies significant above the 90%, 95% and 99% confidence

669 levels, respectively.

670

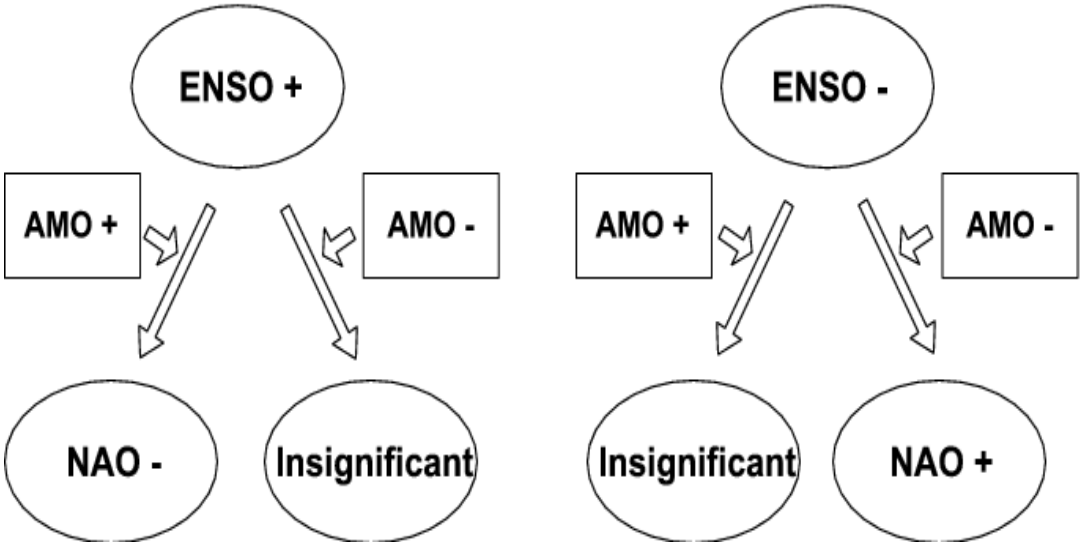

671

672 Figure 11. Schematic for AMO modulation of the ENSO-NAO relationship. "+" and

673 "-" indicates the positive and negative phase, respectively. For instance, ENSO+ and

674 ENSO- represent the positive ENSO phase (i.e., El Niño) and the negative ENSO

675 phase (i.e., La Niña).

676